J|A|C|S
ARTICLES
Published on Web 07/26/2005

Van der Waals Interactions Dominate Ligand−Protein Association in a Protein Binding Site Occluded from Solvent Water

Elizabeth Barratt,[†] Richard J. Bingham,[†] Daniel J. Warner,[‡] Charles A. Laughton,[‡] Simon E. V. Phillips,[†] and Steve W. Homans*,[†]

Contribution from the Astbury Centre for Structural Molecular Biology, School of Biochemistry & Microbiology, University of Leeds, Leeds LS2 9JT, U.K., and Centre for Biomolecular Sciences, School of Pharmacy, University of Nottingham, Nottingham NG7 2RD, U.K.

Received April 28, 2005; E-mail: s.w.homans@leeds.ac.uk

Abstract: In the present study we examine the enthalpy of binding of 2-methoxy-3-isobutylpyrazine (IBMP) to the mouse major urinary protein (MUP), using a combination of isothermal titration calorimetry (ITC), NMR, X-ray crystallography, all-atom molecular dynamics simulations, and site-directed mutagenesis. Global thermodynamics data derived from ITC indicate that binding is driven by favorable enthalpic contributions, rather than a classical entropy-driven signature that might be expected given that the binding pocket of MUP-1 is very hydrophobic. The only ligand−protein hydrogen bond is formed between the side-chain hydroxyl of Tyr120 and the ring nitrogen of the ligand in the wild-type protein. ITC measurements on the binding of IBMP to the Y120F mutant demonstrate a reduced enthalpy of binding, but nonetheless binding is still enthalpy dominated. A combination of solvent isotopic substitution ITC measurements and all-atom molecular dynamics simulations with explicit inclusion of solvent water suggests that solvation is not a major contributor to the overall binding enthalpy. Moreover, hydrogen/deuterium exchange measurements suggest that there is no significant contribution to the enthalpy of binding derived from "tightening" of the protein structure. Data are consistent with binding thermodynamics dominated by favorable dispersion interactions, arising from the inequality of solvent−solute dispersion interactions before complexation versus solute−solute dispersion interactions after complexation, by virtue of poor solvation of the binding pocket.

Introduction

It is now generally accepted that the hydrophobic association of nonpolar solutes in solvent water results from the tendency of the solvent to form a more ordered structure in the vicinity of hydrophobic groups.[1] Hydrophobic groups that are accessible to solvent prior to the association become buried on complex formation with consequent increase in the number of unstructured water molecules. Thus, it might naively be anticipated that the association of hydrophobic groups in aqueous solution would be endothermic and entropy driven, due to the disruption of ordered solvation shells around the interacting species. However, in many instances this thermodynamic signature is not seen, and exothermic binding appears to be the rule rather than the exception in ligand−protein interactions.[2]

The mouse major urinary protein (MUP) is an abundant pheromone-binding protein with a hydrophobic binding cavity, where subtle recognition of a series of related compounds is essential to its biological function,[3,4] and is thus an excellent model system with which to study in detail the thermodynamics of hydrophobic association. Despite the hydrophobicity of the binding site, overall binding thermodynamics for a variety of cognate ligands are found to be strongly enthalpically dominated, with an unfavorable entropic term.[5,6] In an effort to unravel the individual components of the binding process, we recently examined the entropy of binding of small pyrazine-derived ligands 2-methoxy-3-isopropylpyrazine (IPMP) and 2-methoxy-3-isobutylpyrazine (IBMP) to variant I of the major urinary protein, using a combination of isothermal titration calorimetry (ITC), X-ray crystallography, and NMR backbone ^{15}N and methyl side-chain ^{2}H relaxation measurements.[6] While a favorable entropic contribution to binding was found from desolvation of the protein binding site and the ligand, this was counterbalanced by the unfavorable contribution arising from "freezing out" of translational, rotational, and internal degrees of freedom of the ligand. The overall entropic contribution to binding ($T\Delta S \approx -9.4$ kJ/mol for IBMP) was shown to derive principally from the restriction of internal degrees of freedom of the protein on binding.

[†] University of Leeds.
[‡] University of Nottingham.

(1) Frank, H. S.; Evans, M. W. *J. Chem. Phys.* **1945**, *13*, 507−532.
(2) Ross, P. D.; Subramanian, S. *Biochemistry* **1981**, *20*, 3096−3102.
(3) Zidek, L.; Novotny, M. V.; Stone, M. J. *Nature Struct. Biol.* **1999**, *6*, 1118−1121.
(4) Zidek, L.; Stone, M. J.; Lato, S. M.; Pagel, M. D.; Miao, Z. S.; Ellington, A. D.; Novotny, M. V. *Biochemistry* **1999**, *38*, 9850−9861.
(5) Sharrow, S. D.; Novotny, M. V.; Stone, M. J. *Biochemistry* **2003**, *42*, 6302−6309.
(6) Bingham, R.; Bodenhausen, G.; Findlay, J. H. B. C.; Hsieh, S.-Y.; Kalverda, A. P.; Kjellberg, A.; Perazzolo, C.; Phillips, S. E. V.; Seshadri, K.; Turnbull, W. B.; Homans, S. W. *J. Am. Chem. Soc.* **2004**, *126*, 1675−1681.

In the present work we examine the origin of the favorable enthalpic contribution to binding using a combination of ITC, NMR, X-ray crystallography, all-atom molecular dynamics simulations, and site-directed mutagenesis studies.

Materials and Methods

Site-Directed Mutagenesis. The Y120F MUP mutant was generated by PCR-based site-directed mutagenesis using the QuikChange site-directed mutagenesis method (Stratagene). Wild-type plasmid was extracted from SG13009 cells using a QIAprep spin miniprep kit (QIAgen). This plasmid was subjected to mutagenesis using primers GCTGATGGGGCTCTTTGGCCGAGAACC and GGTTCTCGGC-CAAAGAGCCCCATCAGC. This was cycled at 95 °C for 30 s, followed by 16 cycles of 95 °C for 30 s, 55 °C for 1 min, and 68 °C for 4 min. After 16 cycles the reaction was held at 4 °C. Thermal cycling was carried out in an MJ Research PTC200 DNA engine thermal cycler. Dpn1 digestion was performed to degrade the methylated parental strand. The resulting plasmid was used to transform XL1Blue super-competent cells (Stratagene). Plasmid was isolated from the positive transformants and the presence of the mutation verified by di-deoxy terminator DNA sequencing (Lark Scientific). This confirmed the sequence of the mutated plasmid to be identical to that of wild-type[6] except at the position corresponding to residue 120, which was changed from TAT to TTT. The mutated plasmid was transformed into SG13009 cells (QIAgen) for expression and purification.

Preparation and Purification of MUP. Wild-type and Y120F MUP were overexpressed and purified as described in a previous study.[6] Throughout this work the residue numbering of Abbate et al. was used for each protein.[6,7]

X-ray Crystallography. (a) Crystallization and Data Collection. Optimal conditions for crystallization of 55 mM CdCl, 100 mM malate buffer pH 4.9, 18 °C, were based on previously identified conditions.[8] Drops containing 1 μL of Y120F MUP (10 mg/mL) and 1 μL of reservoir solution were equilibrated against reservoir solution by vapor diffusion using the hanging drop method. Crystals of space group $P4_32_12$ grew over a period of 10−20 days. Ligand soaks were conducted by the addition of neat ligand (IBMP) to the reservoir solution to a final concentration of 1 mM. This was then allowed to equilibrate with the drop for 24 h. Crystals were flash-frozen in liquid nitrogen after soaking for 1 min in a cryoprotecting solution consisting of reservoir solution with the addition of 30% (v/v) glycerol and 12 μM IBMP. Data collection of Apo-Y120F-MUP and IBMP-Y120F-MUP was conducted on the laboratory X-ray source, which consisted of a rotating anode generator (RU-H3R, Rigaku), Confocal Max-Flux optics (Osmic), and an R-axis IV++ (Rigaku) image plate detector. Crystals were maintained at 100 K by a cryostream (Oxford Cryosystems). Data were processed and scaled using the programs MOSFLM version 6.10[9] and SCALA.[10]

(b) Structure Determination. The structure of Apo-MUP (PDB accession number 1QY0) was used as the phasing model. After several rounds of automatic positional and thermal factor refinement using CNS[11] interspersed with manual remodeling in the program "O",[12] the final statistics shown in Table 1 were produced. Twelve N-terminal residues including the hexa-His tag, and eight C-terminal residues, were not resolvable due to weak electron density. Crystal coordinates have been deposited in the RCSB protein databank, accession numbers 1YP6 and 1YP7.

Table 1. X-ray Data Collection and Processing Statistics[a]

	free protein	IBMP complex
wavelength (nm)	0.154	0.154
space group	$P4_32_12$	$P4_32_12$
unit cell dimensions (nm)	$a = b = 5.65$	$a = b = 5.38$
	$c = 10.4$	$c = 13.7$
resolution range (nm)	2.8−0.2	5.0−0.18
unique reflections	11 826	18 683
completeness (%)	98.6	95.6
multiplicity	6.4	8.4
R_{sym}[b]	0.09 (0.32)	0.084 (0.37)
R_{work} (R_{free})	19.8 (25.6)	19.4 (22.0)
RMSD from ideal:		
bond length (nm)	0.0011	0.0019
angles (°)	1.6	1.83

[a] Space group for all crystals was $P4_32_12$. [b] Values in parentheses are for highest resolution shell. $R_{sym} = \sum_{hkl}\sum_i(I_i(hkl) - I_{mean}(hkl)/\sum_{hkl}\sum_i(I_i(hkl))$.

Isothermal Titration Calorimetry (ITC) Measurements. ITC experiments were conducted using a MicroCal VP-ITC unit operating at 288, 298, or 308 K. Prior to use, the protein was precipitated with ethanol in order to remove any endogenous ligands and then redissolved, dialyzed against PBS (pH 7.4), and degassed in vacuo. The ligand was dissolved in degassed PBS, and all concentrations were measured by UV absorption (MUP $\epsilon_{280} = 10\,650\ M^{-1}\ cm^{-1}$; IBMP $\epsilon_{220} = 4980\ M^{-1}\ cm^{-1}$) immediately prior to starting the titrations. Titration experiments used protein concentrations of ca. 60 μM. Deuterium isotopic substitution experiments were performed using deuterated PBS (99.96% ^2H), and protein solutions were equilibrated for 72 h at 4 °C in this buffer prior to ITC measurements to ensure isotope exchange. Titrations were performed in duplicate and typically comprised 25 injections (1 × 2 μL followed by 24 × 5 μL) at 4 min intervals. The initial data point was routinely deleted to allow for diffusion of ligand/receptor across the needle tip during the equilibration period. Heats of dilution for each ligand were measured independently and subtracted from the integrated data prior to curve fitting in Origin 5.0 with the standard One Site model supplied by MicroCal, which is based on the Wiseman isotherm:[13,14]

$$\frac{dQ}{d[X]_t} = \Delta H^\circ V_0\left[\frac{1}{2} + \frac{1 - X_R - r}{2\sqrt{(1 + X_R + r)^2 - 4X_R}}\right] \quad (1)$$

where $dQ/d[X]_t$ is the stepwise change in heat of the system normalized with respect to the change in the total concentration of the ligand ($[X]_t$), ΔH° is the standard enthalpy for reaction, V_0 is the effective volume of the calorimeter cell, X_R is the ratio of the total ligand to receptor concentrations at any given point during the titration, and r is defined by

$$\frac{1}{r} = nK_a[M]_t \quad (2)$$

wherein n is the number of binding sites per protein molecule, K_a is the association constant, and $[M]_t$ is the total protein concentration.

Molecular Dynamics Simulations. The starting structure for the protein was taken from the crystal structure of wild-type MUP bound to IBMP, stripped of solvent and all but five well-spaced ligand coordinates, which were then modified to produce five water molecules. The corresponding Y120F mutant was generated by deleting the coordinates for Tyr 120 Oζ and renaming the residue as phenylalanine.

(7) Abbate, F.; Franzoni, L.; Lohr, F.; Lucke, C.; Ferrari, E.; Sorbi, R. T.; Ruterjans, H.; Spinsi, A. *J. Biomol. NMR* **1999**, *15*, 187−188.
(8) Bocskei, Z.; Groom, C. R.; Flower, D. R.; Wright, C. E.; Phillips, S. E. V.; Cavaggioni, A.; Findlay, J. B. C.; North, A. C. T. *Nature* **1991**, *360*, 186−188.
(9) Leslie, A. G. W. In *CCP4 & ESFEACMB Newsletter On Protein Crystallography*; Daresbury Laboratory: Warington, 1992.
(10) CCP4. *Acta Crystallogr.* **1994**, *D50*, 760−763.
(11) Brünger, A. T.; Adams, P. D.; Clore, G. M.; DeLango, W. L.; Gros, P.; Grosse-Kunstleve, R. W.; Jiang, J.-S.; Kuszewski, J.; Nilges, M.; Pannu, N. S.; Read, R. J.; Rice, L. M.; Simonson, T.; Warren, G. L. *Acta Crystallogr.* **1998**, *D54*, 905−921.
(12) Jones, T. A.; Zou, J. Y.; Cowan, S. W.; Kjeldgaard, M. *Acta Crystallogr.* **1991**, *A47*, 110−119.
(13) Wiseman, T.; Williston, S.; Brandts, J. F.; Lin, L. N. *Anal. Biochem.* **1989**, *179*, 131−137.
(14) Turnbull, W. B.; Daranas, A. H. *J. Am. Chem. Soc.* **2003**, *125*, 14859−14866.

The structures were then immersed in a truncated octahedral box containing an additional 6402 TIP3P water molecules.[15] Default ionization states were used when parametrizing the molecule using the Amber ff99 force field,[16] with 13 Na^+ ions being added to neutralize the system.

The two systems containing MUP−IBMP complexes were set up in the same way, but in these systems the ligand coordinates were retained rather than being replaced by water. Parameters for the ligand molecule were generated within the antechamber module of AMBER 7[17] using the general AMBER force field, with partial charges set to fit the electrostatic potential generated at HF/6-31G* by RESP.[18] The calculation of the electrostatic potential was performed according to the Merz−Singh−Kollman scheme[19,20] using Gaussian 98.[21]

All simulations were equilibrated using an extended version of our standard multistage equilibration process,[22,23] involving gentle heating and harmonic restraint reduction over a period of 90 ps. This was followed by unrestrained equilibration of 100 ps. Analysis was performed on data generated through an additional 9.5 ns (solvated cavity) or 5.0 ns (liganded cavity) of unrestrained MD simulation at constant temperature and pressure ($T = 300$ K; $P = 1$ atm) using PMEMD.[24] SHAKE[25] was used to constrain all bonds to hydrogen at equilibrium values, which allowed us to use a 2 fs MD time step. Periodic boundary conditions and the particle-mesh-Ewald method[26] were used to model long-range electrostatic effects. Post-trajectory analysis was completed using the ptraj module of AMBER 7.[17] Theoretical solvation density profiles, assuming uniform and complete occupancy of the binding cavity, were generated by placing a water molecule at every point on a 0.1 Å grid and deleting those that lay within 2.4 Å of any protein atom. The procedure was repeated for 18 snapshots taken at uniform intervals from each MD simulation, and all the data were merged for the plots.

Van der Waals interactions for the water molecules and for the ligand were calculated as follows (see eq 3). The van der Waals component of the total molecular mechanics energy for each of 18 representative snapshots taken from each simulation was calculated (E_{vdW}(system)). The coordinates of the water molecules, or ligand, of interest were then removed, and the energy was recalculated (E_{vdW}(system − molecules)). The difference was then divided (in the case of the water molecules) by the number of such molecules included in the calculation ($N_{molecules}$).

$$E_{vdW}(\text{molecule}) = \frac{[E_{vdW}(\text{system}) - E_{vdW}(\text{system} - \text{molecules})]}{N_{molecules}} \quad (3)$$

H/D Exchange Experiments. Hydrogen/deuterium exchange of the amide protons of MUP was detected by use of conventional NMR ^1H,^{15}H heteronuclear single-quantum correlation (HSQC) experiments. Spectra were acquired at 500 MHz using a single sample of ^{15}N-enriched MUP at a concentration of 1 mM in 50 mM phosphate buffer, pH 7.0, and a probe temperature of 308 K. The sample was divided into two equal aliquots, to one of which was added IBMP to equimolar concentration. Each sample was lyophilized overnight and was resuspended in an equivalent volume of 99.96% D_2O. Initial spectra comprising 16 complex data points and eight transients per increment were acquired within 5 min of insertion of the sample into the cryomagnet (total acquisition time 5 min). Subsequent spectra was acquired after 1 h (128 complex points and eight transients per increment, total acquisition time 40 min). Further spectra were acquired periodically over a period of 24 h. Initial spectra were processed by use of forward linear prediction to 32 complex data points, followed by zero-filling to 256 complex data points in t_1, and cosine-bell squared apodization in both dimensions. Subsequent spectra were processed similarly but without linear prediction.

Scheme 1. Structure of the Ligand 2-Methoxy-3-isobutylpyrazine (IBMP) Used in This Study

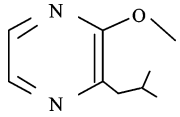

Results

Enthalpic Contribution from Ligand−Protein Hydrogen Bond. The crystal structure of wild-type MUP bound to IBMP and IPMP revealed a single hydrogen bond between the side-chain hydroxyl group of Tyr120 and the ring nitrogen of either ligand.[6] This hydrogen bond may make a substantial favorable contribution to the enthalpy of binding in an environment of low dielectric constant, and values in the region of −25 kJ/mol have been reported.[27,28] Thus, ITC measurements were undertaken on the Y120F mutant of MUP binding to IBMP (Scheme 1) at 308 K for comparison with similar measurements on the wild-type protein reported earlier,[6] in order to assess the thermodynamic contribution to binding from this hydrogen bond.

These data show that the enthalpy of binding is less favorable at 308 K (Table 2) by ∼12 kJ/mol on mutation of Tyr 120 to Phe. However, $T\Delta S$ becomes more favorable by ∼7 kJ/mol, resulting in the "enthalpy−entropy compensation" phenomenon that is commonly observed in biomolecular associations.[29] While this increase in entropy is consistent with the classical hydrophobic effect resulting from the creation of a more hydrophobic binding site upon mutation, it could equally well be attributed in large part to the loss of a degree of freedom about the Tyr $C^{\zeta}-O^{\eta}$ bond.

Crystal Structures of MUP Complexes. To enable a structure-based interpretation of the thermodynamic measurements on Y120F MUP described above, the crystal structures of Y120F MUP both alone and in complex with IBMP were solved, and data collection and processing statistics are shown in Table 1. A comparison of the structures of the uncomplexed protein and the complex with IBMP reveals that the structure of the protein is largely unperturbed following ligand binding. The mean global backbone and side-chain RMSDs between the two structures are 0.15 and 0.56 Å, respectively. Moreover, in either case the binding pocket does not contain any ordered solvent molecules (Figure 1).

(15) Jorgensen, W. L.; Chandrasekhar, J.; Madura, J. D.; Impey, R. W.; Klein, M. L. *J. Chem. Phys.* **1983**, *79*, 926−935.
(16) Wang, J. M.; Cieplak, P.; Kollman, P. A. *J. Comput. Chem.* **2000**, *21*, 1049−1074.
(17) Case, D. A.; et al. *AMBER 7*; University of California: San Francisco, 2002.
(18) Bayly, C. I.; Cieplak, P.; Cornell, W. D.; Kollman, P. A. *J. Phys. Chem.* **1993**, *97*, 10269−10280.
(19) Besler, B. H.; Merz, K. M.; Kollman, P. A. *J. Comput. Chem.* **1990**, *11*, 431−439.
(20) Singh, U. C.; Kollman, P. A. *J. Comput. Chem.* **1984**, *5*, 129−145.
(21) Frisch, M. J.; et al. *Gaussian 98*; Gaussian Inc.: Pittsburgh, PA 1998.
(22) Shields, G. C.; Laughton, C. A.; Orozco, M. *J. Am. Chem. Soc.* **1998**, *120*, 5895−5904.
(23) Shields, G. C.; Laughton, C. A.; Orozco, M. *J. Am. Chem. Soc.* **1997**, *119*, 7463−7469.
(24) Duke, R. E.; Pedersen, L. G.; *PMEMD*; University of North Carolina: Chapel Hill, 2003.
(25) Ryckaert, J. P.; Ciccotti, G.; Berendsen, H. J. C. *J. Comput. Phys.* **1977**, *23*, 327−341.
(26) Darden, T.; York, D.; Pedersen, L. *J. Chem. Phys.* **1993**, *98*, 10089−10092.
(27) Doig, A. J.; Williams, D. H. *J. Am. Chem. Soc.* **1992**, *114*, 338−343.
(28) Daranas, A. H.; Shimizu, H.; Homans, S. W. *J. Am. Chem. Soc.* **2004**, *126*, 11870−11876.
(29) Dunitz, J. D. *Chem. Biol.* **1995**, *2*, 709−712.
(30) Koradi, R.; Billeter, M.; Wuthrich, K. *J. Mol. Graph.* **1996**, *14*, 51.

Table 2. Thermodynamic Parameters for the Binding of 2-Methoxy-3-isobutylpyrazine (IBMP) to Wild-Type MUP and Y120F MUP Derived from ITC Experiments

ligand	ΔH° (kJ/mol)[a]	stoichiometry	$T\Delta S^\circ$ (kJ/mol)	ΔG° (kJ/mol)	K_d (μM)
wild-type[b]					
308 K	-47.89 ± 0.86	1.01 ± 0.02	-9.39 ± 0.87	-38.5 ± 0.11	0.30 ± 0.01
Y120F					
H_2O					
288 K	-25.76 ± 0.88[c]	0.97 ± 0.02	9.12 ± 0.89	-34.89 ± 0.17	0.47 ± 0.03
298 K	-31.44 ± 0.79	1.01 ± 0.02	3.87 ± 0.80	-35.31 ± 0.1	0.65 ± 0.03
308 K	-35.90 ± 1.05	0.98 ± 0.03	-2.29 ± 1.05	-33.61 ± 0.12	1.99 ± 0.1
D_2O					
308 K	-34.21 ± 1.05	0.98 ± 0.02	-0.4 ± 1.05	-33.82 ± 0.12	1.84 ± 0.09

[a] Values are expressed as the mean of two measurements. [b] Values taken from Bingham et al.[6] [c] Errors were determined from duplicate experiments by error propagation.

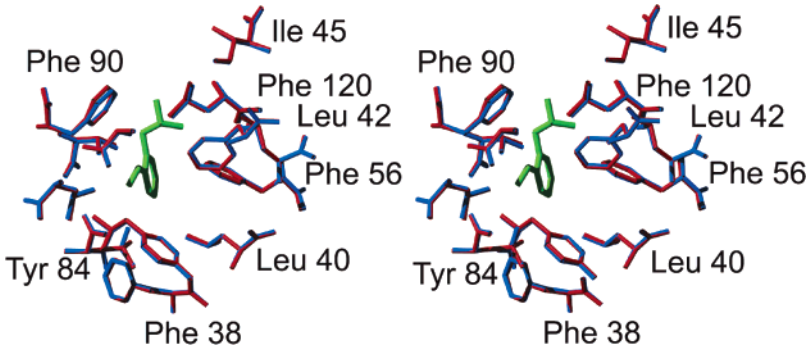

Figure 1. Stereoview of the superimposition of the ligand binding sites observed in crystal structures of uncomplexed Y120F MUP (blue) and Y120F MUP (red) in complex with IBMP (green). No ordered water molecules are observable within the binding site in either structure. Figure prepared using MOLMOL.[30]

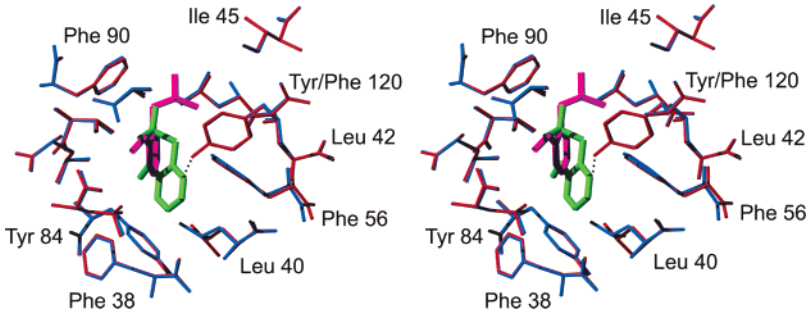

Figure 2. Stereoview of the superimposition of the ligand binding sites observed in crystal structures of complexes of wild-type MUP (red) with IBMP (green) and Y120F MUP (blue) with IBMP (magenta). The ligand−protein hydrogen bond observed in the wild-type protein is indicated by the dotted line. Figure prepared using MOLMOL.[30]

Details of the binding sites of wild-type MUP[6] and Y120F MUP bound to IBMP are shown in Figure 2. It can be seen that the Y120F mutation maintains the integrity of the binding pocket, with only minor reorientation of the side chains of Leu 40 and Leu 42. The loss of the hydrogen bond subtended by Tyr 120 gives rise to a significant relocation of IBMP in the binding pocket of the mutant to an alternative energy minimum. It is thus clearly not possible to determine directly the thermodynamic contribution from this hydrogen bond from the difference in binding enthalpy between the wild-type and mutant proteins, but this value clearly places a lower limit to this contribution (i.e. −12 kJ/mol). Despite the loss of the ligand−protein hydrogen bond, binding is however still strongly enthalpically driven, indicating that additional factors dominate binding thermodynamics.

Solvation Contribution to Binding Enthalpy. In considering the additional factors that contribute to binding thermodynamics, it is convenient to represent the overall binding process in terms of a conventional Born−Haber cycle (Scheme 2). Since

Scheme 2. Born−Haber Cycle for Ligand L Binding to Protein P, Showing the Relationship between the Observed Enthalpy of Binding, ΔH_{obs}, the "Intrinsic" (Solute−Solute) Enthalpy of Binding, ΔH_i, and the Solvation Enthalpies of the Unbound (ΔH_{su}) and Bound (ΔH_{sb}) Species

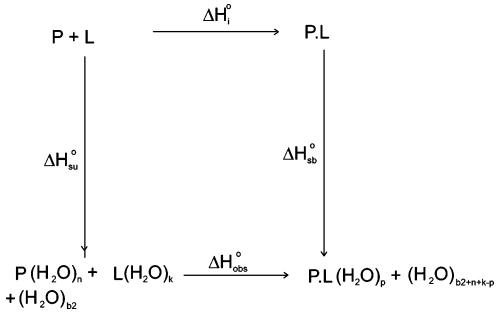

H is a state function, the observed enthalpy of binding is given by

$$\Delta H^\circ_{obs} = \Delta H^\circ_i + \{\Delta H^\circ_{sb} - \Delta H^\circ_{su}\} \quad (4)$$

where ΔH°_i is the "intrinsic" solute−solute (ligand−protein)

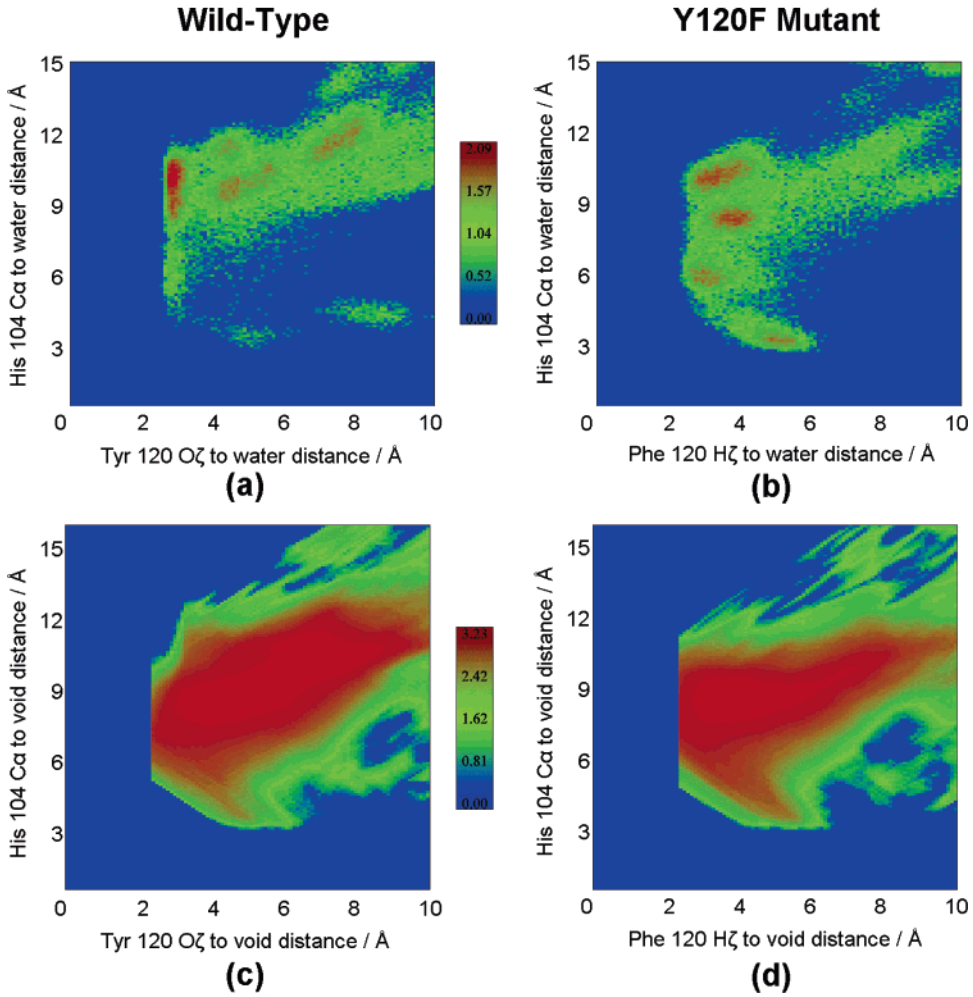

Figure 3. Water distributions in the binding cavity of MUP, as a function of distance from two key residues. (a) Data from 9500 snapshots of the MD simulation of wild-type protein, and (b) the same for the Y120F mutant simulation. (c) For comparison, the distribution that would result from uniform water occupancy of the whole cavity of the wild-type protein (averaged over 18 equally spaced snapshots from the MD trajectory), and (d) the same for the Y120F mutant. The color coding is by the log of the number of observations in each 0.1 Å^2 bin.

binding enthalpy, and the quantity in curly braces is a "solvation term" comprised of the solvation enthalpy of the complex, $\Delta H°_{sb}$, and the solvation enthalpy prior to the association, $\Delta H°_{su}$. Chervenak and Toone demonstrated that it is possible to determine experimentally the solvation term in eq 4 by use of thermodynamic isotope substitution techniques where deuterium is substituted for protium.[31] In general, solvent isotopic substitution results in a less negative enthalpy of binding due to stabilization of the unbound state relative to the bound state, and the difference between these values, $\Delta\Delta H$, is a measure of the contribution to the enthalpy of binding due to solvent reorganization (i.e. desolvation of the protein and ligand upon association). In the present study we have utilized this approach by measurement of the thermodynamics of binding of IBMP to Y120F MUP in deuterated solvent at 308 K (see methods). The standard enthalpy of binding thus obtained was identical, within experimental error, with that obtained in protonated solution (Table 2), which suggests that the solvation contribution to the enthalpy of binding is very small or negligible; i.e., solvent water within the binding pocket and surrounding the ligand prior to the association is released into an environment that is enthalpically neither more nor less favorable following association. However, since the observed enthalpy difference of binding in H_2O versus D_2O represents only ~10% of the solvation contribution, this approach is susceptible to substantial error.

Molecular Dynamics Simulations of Protein Solvation. Given the limitations of the thermodynamic isotope substitution approach, the behavior of solvent water molecules in the binding pocket of Y120F MUP was examined further by use of all-atom molecular dynamics simulations with explicit inclusion of solvent water molecules. Initial coordinates were generated for both wild-type MUP and Y120F MUP from the crystal structures of the complexes with IBMP, from which IBMP was removed and replaced with five solvent water molecules. Solvent density was then examined over the course of two 9.5-ns simulations. The binding cavity is roughly "sock" shaped, with Tyr/Phe 120 located at the "heel" and residue His 104 at the "toe". Shown in Figure 3 are plots of solvent density with respect to distance from Tyr 120 Oζ (or Phe 120 Hζ) versus His 104 Cα. Hydrogen bonding between water and the side-chain hydroxyl group of Tyr 120 can be detected from the high water density at short Tyr 120−water distances (Figure 3a) in comparison with the more diffuse density in the Y120F mutant simulation (Figure 3b). The effect of hydrogen bonding to Tyr 120 apparently inhibits access of solvent to the "toe" of the hydrophobic pocket, whereas greater density inside the cavity

(31) Chervenak, M. C.; Toone, E. J. *J. Am. Chem. Soc.* **1994**, *116*, 10533−10539.

is apparent for the Y120F mutant, as is apparent from a peak in density at Phe120 Hζ−water and His 104 Cα−water distances (∼5 Å). To see to what extent these solvation density patterns reflect how water molecules actually choose to occupy and distribute themselves in the cavity, as opposed to features due purely to the shape of the cavity itself, and how this alters between the wild-type and F120 mutant structures, we also calculated how these solvation maps would look if water molecules actually completely and uniformly filled the cavity in each case. The results for the wild-type protein are shown in Figure 3c, and for the mutant in Figure 3d.

The simulations reveal that the wild-type and mutant binding sites contain on average 3.46 and 4.07 water molecules, respectively. Note that each simulation began with five molecules within the site, so in the initial phase of each simulation there is a net expulsion of water from the site. From calculations of the average binding-site cavity volume, these figures equate to average solvent densities within the binding site of 0.21 and 0.23 g cm^{-3} for wild-type and mutant proteins, respectively. Though Figure 3 clearly shows that solvent density peaks exist, their diffuse nature and low occupancy are in agreement with the X-ray data. Comparing the actual (panels a and b) against theoretical uniform (panels c and d) solvent distributions, it is clear that differences between the solvent distributions in the wild-type and mutant proteins are not related to gross changes in the cavity shape or size, and that large portions of the cavity that are theoretically available to solvent show very low occupancy indeed.

Taken together, the data above are in remarkable contrast with the results of an earlier study by Connelly et al. on the binding of the macrocycles FK506 and rapamycin to the FK506 binding protein.[32] As in the present study, a feature of these protein−ligand complexes is a hydrogen bond between a binding-site tyrosine in FK506 (Tyr-82 Hζ) and the ligand. However, in a Y82F mutant of FK506, Connelly et al. recorded a significantly more *favorable* binding enthalpy to FK506 and rapamycin compared with the wild-type protein ($\Delta\Delta H° = -17.6$ and −12.7 kJ/mol, respectively). Moreover, significantly less favorable binding enthalpies were recorded on substitution of H_2O with D_2O for the Y82F mutant ($\Delta\Delta H° = 18.0$ and 12.1 kJ/mol for FK506 and rapamycin, respectively). These observations were rationalized by noting that the crystal structure of the unliganded protein shows two solvent water molecules ordered around the Tyr-82 hydroxyl group. The more favorable binding enthalpy in the Y82F mutant was suggested to arise from the desolvation of the latter group, which was considered to be a highly unfavorable enthalpic process. The reverse trend in binding enthalpy observed with an analogous mutation in the present study thus lends support to the absence of ordered water molecules within the binding site.

Enthalpic Contribution to Binding from Protein Desolvation The above data, taken together, show that while the MUP binding site is occluded from solvent, water molecules nonetheless exist within the binding pocket of the uncomplexed protein. These water molecules are disordered, and thus H-bonding to neighboring water molecules in the bulk solvent on displacement might make a significant favorable contribution to the observed binding enthalpy. The magnitude of this contribution is very difficult to assess accurately in terms of H-bonding economy, given the disorder in the binding pocket, and consequently the numbers and fractional occupancies of H-bonds cannot be assessed with any degree of confidence. However, estimates are available for the enthalpy of formation of a hydrogen bond in a protein−solvent lattice based on measurements in the vapor phase, which suggest an upper limit of −12 to −25 kJ/mol.[33,34] Assuming a fractional occupancy for each hydrogen bond of 50% in bulk solvent and ("worst-case") 0% within the binding pocket, and given the average number of solvent molecules within the binding pocket derived from the above MD simulations, a net favorable enthalpic contribution for binding of −25 to −50 kJ/mol can be derived.

Enthalpic Contribution to Binding from Ligand Desolvation. It is clear from eq 4 and Scheme 2 that the solvation term $\{\Delta H°_{sb} - \Delta H°_{su}\}$ is governed not only by protein desolvation, but also by ligand desolvation, on complex formation. While the contribution to binding enthalpy from ligand solvation effects should also be apparent in isotope substitution experiments, quantitation is not straightforward, given the above-mentioned scope for significant error in these measurements. Nonetheless, solvation enthalpies of small, hydrophobic solutes are invariably negative at physiological temperature,[35] and thus ligand solvation will result in an *unfavorable* contribution to the enthalpy of binding. To the extent that ligand binding represents a desolvation process, the enthalpic contribution to this process can be estimated from the solvation enthalpy of the ligand. To the best of our knowledge, the solvation enthalpy of IBMP has not been reported. However, data exist for related molecules. The solvation enthalpy of pyridine is −49.8 kJ/mol,[36] and the solvation enthalpy of pyrazine can be calculated as −34.5 kJ/mol from the reported enthalpies of solution[37] and vaporization.[38] Given the reported solvation enthalpies of 2-ethylpyridine (−55.7 kJ/mol) and 4-methoxypyridine (−59.1 kJ/mol), a value of ∼ −50 kJ/mol for the solvation enthalpy of IBMP can be estimated. Thus, the unfavorable enthalpic contribution to binding of IBMP to MUP from ligand desolvation (+50 kJ/mol) may approximately compensate for the favorable contribution arising from protein desolvation, which would provide a tentative explanation for the absence of solvent isotope substitution effects on binding thermodynamics. Evidence that desolvation does appear to contribute to binding thermodynamics in the sense of the classical hydrophobic effect is apparent from a significant negative change in heat capacity, ΔC_p, for the association[39] (−0.51 ± 0.03 kJ/mol·K) determined from the temperature dependence of the enthalpy of binding of IBMP to Y120F MUP (Table 2). However, there is increasing evidence that hydrophobic interactions are not the only possible source of such effects.[40]

Enthalpic Contribution to Binding from Solute−Solute Interactions. If the favorable enthalpy of binding of IBMP to

(32) Connelly, P.; Aldape, R. A.; Bruzzese, F. J.; Chambers, S. P.; Fitzgibbon, M. J.; Fleming, M. A.; Itoh, S.; Livingston, D. J.; Navia, M. A.; Thomson, J. A.; Wilson, K. P. *Proc. Natl. Acad. Sci.* **1994**, *91*, 1964−1968.
(33) Rose, G. D.; Wolfenden, R. *Annu. Rev. Biophys.* **1993**, *22*, 381−415.
(34) Cooper, A. *Biophys. Chem.* **2000**, *85*, 25−39.
(35) Ben-Naim, A.; Marcus, Y. *J. Chem. Phys.* **1984**, *81*, 2016−2027.
(36) Cabani, S.; Gianni, P.; Mollica, V.; Lepori, L. *J. Solution Chem.* **1981**, *10*, 563−595.
(37) Spencer, J. N.; Holmboe, E. S.; Kirshenbaum, M. R.; Barton, S. W.; Smith, K. A.; Wolbach, W. S.; Powell, J. F.; Chorazy, C. *Can. J. Chem.* **1982**, *60*, 1183−1186.
(38) Steele, W. V.; Chirico, R. D.; Knipmeyer, S. E.; Nguyen, A. *J. Chem. Eng. Data* **2002**, *47*, 689−699.
(39) Kauzmann, W. *Adv. Protein Chem.* **1959**, *14*, 1−63.
(40) Cooper, A. *Biophys. Chem.* **2005**, *115*, 89−97.

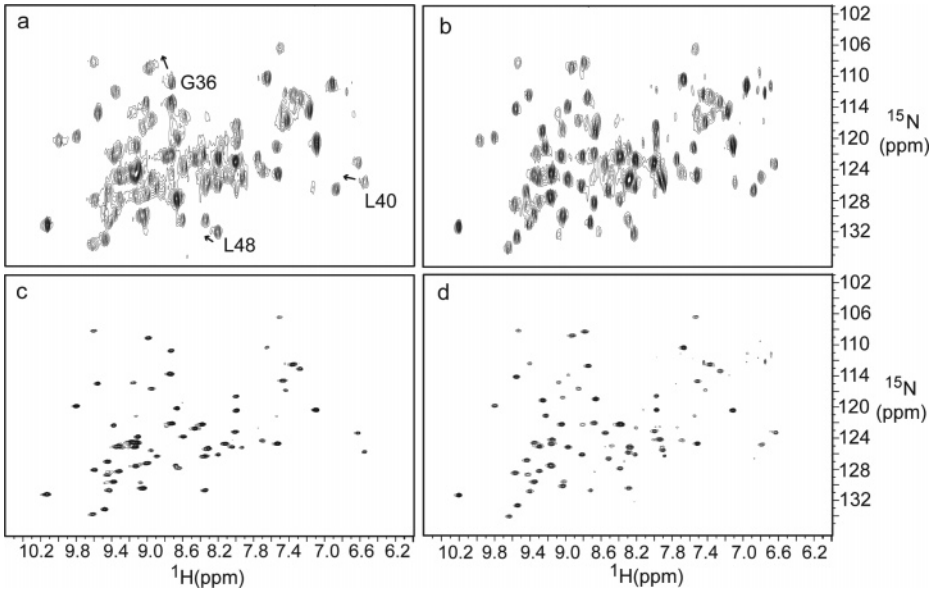

Figure 4. Amide proton hydrogen/deuterium exchange in uncomplexed MUP (a,c) versus MUP in complex with IBMP (b,d) monitored by $^{1}H-^{15}N$ NMR HSQC spectra. Spectra a and b were acquired 5 min after addition of D_2O to the lyophilized, protonated material (total acquisition time 5 min), and spectra c and d were acquired 1 h later (total acquisition time 40 min). Increased line widths in spectra a and b with respect to those in spectra c and d reflect the limited digital resolution in the F_1 (^{15}N) dimension dictated by the requirement for rapid acquisition of the former. Several typical resonance shifts of binding-site residues upon complexation are indicated by arrows in panel a. Spectra acquired over a subsequent period of 24 h are essentially identical to spectra c and d (data not shown).

MUP does not derive from solvent reorganization, from where does it derive? An intriguing possibility, proposed by Williams and co-workers,[41] suggests that favorable enthalpic contribution to binding is a consequence of the "tightening" of the protein around the ligand, i.e., a strengthening of existing nonbonded interactions, mainly within the protein, rather than de novo contributions from interactions at the protein−ligand interface. A number of observations suggest that this mechanism offers a very small or negligible contribution to the favorable enthalpy of binding of IBMP to MUP. First, previous work from our laboratory has shown that, while the entropic contribution from the side chains of methyl-containing residues within the binding pocket of MUP becomes less dynamic on ligand binding, side chains distal to the binding pocket become more dynamic, resulting in a very small entropic contribution to binding from protein degrees of freedom.[6] It follows, therefore, that any enthalpic contribution would be largely compensated in a similar manner. Second, a comparison of the crystal structures of either wild-type MUP obtained previously[6] or Y120F MUP obtained in the present study shows no evidence of structural "tightening" on ligand binding. However, it is proposed that such structural tightening can arise from very small changes in structure throughout the protein that may not be observable in crystal structures.[41] In this regard, although a number of ^{15}N and $^{1}H^{N}$ chemical shifts are observed in $^{1}H-^{15}N$ HSQC spectra of uncomplexed MUP in comparison with the complex with IBMP, these shift changes are invariably associated with residues in or near the binding pocket. The exquisite sensitivity of the chemical shift to environment would ensure that significant shifts are distributed throughout the protein if global structural changes occur on ligand binding. Finally, it has been suggested by Williams et al.[41] that a suitable reporter of structural "tightening" is reduced H/D exchange of amide protons on ligand binding. In contrast, we find no difference in H/D exchange under these circumstances over time scales ranging from 5 min to 1 h, extending to at least 24 h (Figure 4).

Over two decades ago, Ross and Subramanian,[2] on the basis of the limited thermodynamic data that were available at that time, noted that the thermodynamics of many "hydrophobic" associations were enthalpy driven. They endeavored to explain this trend in terms of a conceptual model involving hydrophobic association in the conventional sense, i.e., as a result of the tendency of water to form a more ordered structure in the vicinity of nonpolar hydrocarbon groups, giving rise to a favorable entropy and unfavorable enthalpy of binding. Moreover, in addition to the classical hydrophobic interaction, they suggested that the hydrophobically associated species participate in further interactions following the association, which are dominated by van der Waals and hydrogen-bonding interactions, and which are associated with dominant negative signs for the enthalpy and entropy of the association. Despite these observations, in general it has been surmised that hydrogen-bonding and van der Waals interactions are not a dominant driving force for ligand−protein association, since ligand−protein interactions of this nature are "exchanged" for similar solute−solvent interactions that pre-exist prior to the association. In the case of MUP, however, we have demonstrated above that the protein binding site is poorly solvated, and hence the solvent will be unable to compensate for the gain in solute−solute dispersion interactions. This has been experimentally demonstrated for the interaction of small organic molecules where the geometry of the binding pocket prevents solvation,[42,43] and thus similarly van der Waals interactions are expected to present a favorable enthalpic contribution to binding of IBMP and other small molecules to MUP. The magnitude of this contribution can readily be estimated from MD simulations described above.

(41) Williams, D. H.; Stephens, E.; O'Brien, D. P.; Zhou, M. *Angew. Chem., Int. Ed.* **2004**, *43*, 6596−6616.

(42) Chapman, K. T.; Still, W. C. *J. Am. Chem. Soc.* **1989**, *111*, 3075−3077.
(43) Hunter, C. A. *Angew. Chem., Int. Ed.* **2004**, *43*, 5310−5324.

From the original simulations of the protein with a solvated cavity, we calculated average solvent−protein van der Waals interaction energies for each of the solvent molecules within the pocket (−1.1 and −1.42 kJ/mol for wild-type and Y120F mutant protein respectively). From simulations of the protein−ligand complex (see methods), we calculated the average ligand−protein van der Waals interaction energy of −107.9 and −106.9 kJ/mol for wild-type and Y120F mutant protein, respectively. Given that the average number of water molecules in the binding pocket prior to association is known (see above), a favorable van der Waals interaction energy upon ligand binding of ∼100 kJ/mol is therefore predicted in each case. It must be emphasized that this energy is only a rough estimate, but it does illustrate that the gain in solute−solute dispersion interactions can be very large in a poorly solvated binding pocket prior to the association. It is notable that, very recently, similar large stabilization energies have been predicted inside the hydrophobic core of rubredoxin using rigorous correlated ab initio quantum chemical calculations.[44]

It must be emphasized that our conclusions are not necessarily at variance with the "classical" view of the hydrophobic effect. Rather, they may offer an explanation for the fact that many "hydrophobic associations" in solution do not possess the anticipated entropy-driven thermodynamic signature. In contrast to the IBMP−MUP interaction studied here, the binding of a series of hydrophobically modified benzamidinium chloride inhibitors to trypsin is strongly entropy driven at a number of temperatures.[45] Notably, the trypsin binding site is a cleft that is presumably heavily solvated. Thus, we suggest that, in general, the characteristic thermodynamic signature of hydrophobic association in solution will depend on the degree of solvation of the binding pocket. The architecture of this pocket would appear to be at least as important as hydrophobicity in determining the relative contribution of enthalpic versus entropic effects in biomolecular associations.[46−48] This leads to the intriguing question of how the architecture of a protein binding site influences its solvation. We are actively pursuing this line of enquiry.

Acknowledgment. This work was supported by BBSRC, grant no. 24/B19388 to S.W.H., 24/SB11269 to S.E.V.P., and 00A1E06372 to C.L., and by The Wellcome Trust, grant no. 062164.

Supporting Information Available: Complete refs 17 and 21. This material is available free of charge via the Internet at http://pubs.acs.org.

JA0527525

(44) Vondrasek, J.; Bendova, L.; Klusak, V.; Hobza, P. *J. Am. Chem. Soc.* **2005**, *127*, 2615−2619.
(45) Talhout, R.; Villa, A.; Mark, A. E.; Engberts, J. *J. Am. Chem. Soc.* **2003**, *125*, 10570−10579.
(46) Isbister, B. D.; St. Hilaire, P. M.; Toone, E. J. *J. Am. Chem. Soc.* **1995**, *117*, 12877−12878.
(47) Luque, I.; Freire, E. *Proteins* **2002**, *49*, 181−190.
(48) Vega, S.; Kang, L. W.; Velazquez-Campoy, A.; Kiso, Y.; Amzel, L. M.; Freire, E. *Proteins* **2004**, *55*, 594−602.